Available online at
https://jcrinn.com/
https://crinn.conferencehunter.com/

Journal of Computing Research and Innovation 10(2) 2025

Journal of Computing Research and Innovation

Hydrological Risk Assessment of the Johor River: Flood Frequency Analysis with L-Moments

Nur Hanida Othman[1], Basri Badyalina[2*], Sheril Haiza Shah Izan[3], Ani Shabri[4], Muhammad Fadhil Marsani[5], Fatin Farazh Ya'acob[6]

[1,3]*Faculty of Computer and Mathematical Sciences, Universiti Teknologi MARA Negeri Sembilan Branch, Seremban Campus, 70300 Negeri Sembilan, Malaysia.*
[2]*Faculty of Computer and Mathematical Sciences, Universiti Teknologi MARA Johor Branch, Segamat Campus, 85000 Johor, Malaysia.*
[4]*Department of Mathematical Sciences, Faculty of Science,Universiti Teknologi Malaysia, 81310, Johor, Malaysia.*
[5]*School of Mathematical Sciences, Universiti Sains Malaysia, 11800 Minden, Penang, Malaysia.*
[6]*Faculty of Business and Management, Universiti Teknologi MARA Johor Branch, Segamat Campus, 85000 Johor, Malaysia.*

ARTICLE INFO

Article history:
Received 29 April 2025
Revised 4 July 2025
Accepted 16 August 2025
Published 1 September 2025

Keywords:
L-Moments
Generalized Pareto
Return Period
Hydrological Modelling
Flood Frequency Analysis
Johor River

DOI:
10.24191/jcrinn.v10i2.527

ABSTRACT

Flooding remains one of the most significant hydrological hazards in Malaysia, particularly within the Johor River Basin. This study conducts a Flood Frequency Analysis (FFA) using the L-Moment method to identify the most suitable probability distribution for modelling annual maximum streamflow at the Kahang River station. A 45-year dataset (1978-2022) was analyzed using three candidate distributions: Generalized Logistic (GLO), Generalized Pareto (GPA), and Pearson Type-III (PE3). The L-Moment Ratio Diagram (LMRD), alongside statistical performance metrics such as *MAE*, *RMSE*, *MAPE*, *RMSPE*, R^2 and Euclidean Distance was employed to evaluate model accuracy. Results reveal that the GPA distribution provides the best fit as it provides smallest value of *MAE, MAPE, RMSPE* and Euclidean Distance, demonstrating superior accuracy in predicting extreme flood events, particularly for high return periods. The study offers critical insights for flood risk assessment, infrastructure planning, and early warning system development in the region. Lastly, it provided researchers with flood analysis methods using L-moments and extreme value distributions.

1. INTRODUCTION

Flood is one of the most destructive natural disasters, with severe socio-economic impacts globally. In Malaysia, the Johor River basin is highly flood-prone due to its tropical climate, featuring heavy rainfall during the northeast monsoon (November-February). High temperatures (24º-32ºC) and year-round humidity further increase flood risks, making Johor particularly vulnureable to extreme weather. Over past

[2*] Corresponding author. *E-mail address*: basribdy@uitm.edu.my
https://doi.org/10.24191/jcrinn.v10i2.527

20 years, major flood such as those in 2006-2007, 2011 and 202 have caused widespread displacement, damage to infrastructure and livelihood disruptions (Ahmad et al., 2020)

To assess flood risks, hydrologists use various Flood Frequency Analysis (FFA) models, the key method for studying extreme river flows and predicting recurrence intervals (Hamed & Rao, 2019; Jan et al., 2016). FFA methods evolved to incorporate historical data, censored peaks, and outlier tests, significantly improving flood quantile estimation (Stedinger, 1993; Hamed & Rao, 2019; Ali & Rahman, 2022). Early foundational work (Fakhru'l-Razi et al., 2020) by Todd (1957) and Linsley (1986) established streamflow analysis principles, while later Moughamian et al. (1987) advanced the distribution methods.

Advanced statistical techniques, such as L-moments presented an efficient alternative for the estimation of extreme hydrologic data (Badyalina et al., 2021). The reason to utilized the L-Moment in this study is because L-moments are less sensitive to outliers and produce better parameter estimation of probability distributions like the Generalized Logistic (GLO), Generalized Pareto (GPA) and Pearson Type-III (PE3) distributions (Marsani et al., 2022; Hassim et al., 2022). By applying these methods to historical records of floods in the Johor River, it was then feasible to enhance the description of the frequency and size of flood events and can refine the precision of flood risk predictions.

Studies in Johor rivers, such as the Sayong River, Segamat River, and Johor's Region III confirm GLO's superior fit for peak flow data (Zamani et al., 2024; Badyalina et al., 2021; Che Ilias et al., 2021). Meanwhile, GPA outperformed other distributions in the Segamat River (Romali & Yusop, 2017) and matched regional L-moments in flood-prone areas like Northern Iran (Adhami, 2024). The Pearson Type-III (P3) distribution handles asymmetric data through shape, scale, and location parameters, offering versatility for skewed flood data (Zhang et al., 2012). Recent studies highlight its superiority in the Johor River Basin (Jafry et al., 2023; Badyalina et al., 2022) and moderate-skew environments (Turhan, 2022), even outperforming GLO and GPA in some cases (Valentini et al., 2024). Though less common in Johor, PE3 shows promise for regional adaptation.

Hence, this study aims to improve flood risk assessment for Johor River by applying L-Moments and extreme value distributions (Generalized Pareto (GPA), Generalized Logistic (GLO) and Pearson Type-III (PE3)) to analyse historical flood data from Sungai Kahang station. The advantages of using each distribution are for GLO, it has satisfactory estimation of extreme flood events as it is able to capture tail behaviour well (Hamed & Rao, 2019). GPA is effective for heavy-tailed data meanwhile PE3 distribution can augment the data input from positively skewed data to negative skewed data depending on the location parameter, the PE3 distribution has great utility across many real-world scenarios.

The research will identify the most accurate distribution for modelling flood frequency, estimate return periods for extreme events, and provide actionable insights for flood management agencies like Department of Irrigation and Drainage Malaysia (DIDM). While the findings will enhance early warning systems and infrastructure planning, limitations include time constraints restricting long-term climate analysis and data accessibility challenges affecting prediction precision. The methodology used in this research is presented in methodology section, covering the study area description, probability distributions, and evaluation criteria for distributions performance.

2. METHODOLOGY

2.1 Study area

This study analyzes flood patterns and extreme streamflow events in Johor, Malaysia, using historical data f This study analyzes flood patterns and extreme streamflow events in Johor, Malaysia, using historical data from a river station which is Kahang River (Station ID 2235401, coordinates 2°17'42"N 103°34'39"E). The research utilizes a 45-year dataset from 1978 until 2022 of annual maximum streamflow (in m^3/s) obtained from the Department of Irrigation and Drainage Malaysia (DIDM). This study focuses on annual

https://doi.org/10.24191/jcrinn.v10i2.527

streamflow data, excluding weekly and monthly measurements from the analysis. These long-term discharge records, collected from the gauging station shown in Fig. 1., hydrological stations in Johor including Kahang River.

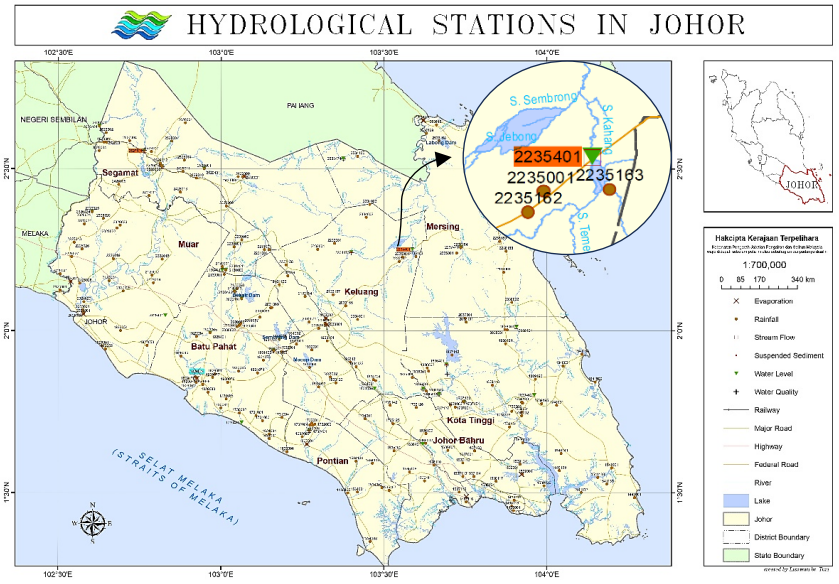

Fig. 1. Location of Kahang River

Source: Department of Irrigation and Drainage Malaysia

2.2 Gringorten plotting position

Gringorten's formula is commonly used to plot a set of ordered observations in a simpler format. According to Gringorten (1963), the Gringorten plotting position is used to find the optimal plotting position. This method is especially helpful in proving the efficiency of the plotting position, even when the sample size is less than 20. The Gringorten plotting position is calculated using the following formula:

$$P_i = \frac{i - 0.44}{n + 0.12} \tag{1}$$

where P_i is the plotting position for the i_{th} value, i is the rank of the value in the ordered dataset, and n is the sample size of the data.

2.3 L-Moments

L-moments (LMO), which are derived from probability-weighted moments (PWM), are commonly employed in hydrology for analysing extreme events like floods and droughts. They outperform traditional statistical methods by being less affected by outliers and working well with small datasets (Hamed & Rao, 2019). L-moments provide reliable estimates of distribution parameters, improving flood frequency analysis and water management decisions. Hosking (1990) developed the PWM approach that forms the basis for L-moment calculations. Assume $x_{1:n} \leq x_{2:n} \leq \cdots \leq x_{n:n}$ represented the data in specific order with a sample size of n. Landwehr (1979) outlined the L-Moment method's unbiased sample estimator by the following formula:

https://doi.org/10.24191/jcrinn.v10i2.527

$$b_r = \frac{1}{n}\binom{n-1}{r}^{-1} \sum_{i=r+1}^{n} \binom{i-1}{r} x_{i:n} \tag{2}$$

The first four elements of an unbiased sample estimator are listed below:

$$b_0 = \frac{1}{n}\sum_{i=1}^{n} x_{i:n} \tag{3}$$

$$b_1 = \frac{1}{n}\sum_{i=2}^{n} \frac{(i-1)}{(n-1)} x_{i:n} \tag{4}$$

$$b_2 = \frac{1}{n}\sum_{i=2}^{n} \frac{(i-1)(i-2)}{(n-1)(n-2)} x_{i:n} \tag{5}$$

$$b_3 = \frac{1}{n}\sum_{i=2}^{n} \frac{(i-1)(i-2)(i-3)}{(n-1)(n-2)(n-3)} x_{i:n} \tag{6}$$

Meanwhile, the first four sample estimates for L-Moments listed as:

$$l_1 = b_0 \tag{7}$$

$$l_2 = 2b_1 - b_0 \tag{8}$$

$$l_3 = 6b_2 - 6b_1 + b_0 \tag{9}$$

$$l_4 = 20b_3 - 30b_2 + 12b_1 + b_0 \tag{10}$$

Hence, the samples of L-Moment ratio are addressed as follows:

$$t_2 = \frac{l_2}{l_1} \tag{11}$$

$$t_3 = \frac{l_3}{l_2} \tag{12}$$

$$t_4 = \frac{l_4}{l_2} \tag{13}$$

L-moments summarize streamflow data, where l_1 (L-location) represents the central value, l_2 (L-scale) measures data variability (higher values indicate greater spread), and t_2 (L-CV) quantifies relative variation. L-skewness (t_3) and L-kurtosis (t_4) describe tail and peak behavior. Table 1 evaluates three distributions (GLO, GPA, PE3) for flood frequency analysis, showing their formulas ($x(F)$ = quantile at non-exceedance probability $F = 1 - 1/T$, where T = return period). Each distribution is defined by location (ζ), scale (α), and shape (k) parameters, which determine its fit to the data.

https://doi.org/10.24191/jcrinn.v10i2.527

Table 1. Estimated distribution parameters using the L-Moments technique

Dist	Cumulative Density Function	Parameter Estimation
GLO	$x(F) = \hat{\xi} + \frac{\hat{\alpha}}{\hat{k}}\left(1 - \left(\frac{1-F}{F}\right)^{k}\right)$	$\hat{k} = -t_3$ $\hat{\alpha} = \frac{l_2}{\Gamma(\hat{k})\left[\Gamma(1-\hat{k}) - \Gamma(2-\hat{k})\right]}$ $\hat{\xi} = l_1 - \frac{\hat{\alpha}}{\hat{k}} + \hat{\alpha}\Gamma(\hat{k})\Gamma(1-\hat{k})$
GPA	$x(F) = \hat{\xi} + \frac{\hat{\alpha}}{\hat{k}}\{1 - [1-F]^{k}\}$	$\hat{k} = \frac{1-3t_3}{1+t_3}$ $\hat{\alpha} = l_2(\hat{k}+1)(\hat{k}+2)$ $\hat{\xi} = l_1 - \frac{\hat{\alpha}}{\hat{k}} + \frac{\hat{\alpha}}{\hat{k}(\hat{k}+1)}$
PE3	$x(F) = \hat{\xi}\hat{k} + K_T\sqrt{\hat{\xi}^2\hat{k}}$ where $K_T = \frac{2}{C_s}\left[\left\{\frac{C_s}{6}\left(\Phi^{-1}[1-F] - \frac{C_s}{6}\right) + 1\right\}^{3} - 1\right]$ $C_s = \frac{2}{\sqrt{\hat{k}}}$	$\hat{k} = 0.0127331632 + \frac{1.0246130369}{3p(t_3)^2} - \frac{1.0246130369}{3p(t_3)^2} - \frac{0.0024863669}{(3p(t_3)^2)^2} + \frac{0.0001169073}{(3p(t_3)^2)^3} - \frac{0.0000027751}{(3p(t_3)^2)^4} + \frac{0.000000323}{(3p(t_3)^2)^5} - \frac{0.000000001}{(3p(t_3)^2)^6}$ $\hat{\alpha} = \frac{l_2}{2S_1(\hat{k}) - \hat{k}}$ $S_1(\hat{k}) = \int_0^{\infty}\left[\int_0^{x}\frac{1}{\Gamma(\hat{k})}t^{\hat{k}-1}e^{-t}\,dt\right]^{\gamma}\frac{1}{\Gamma(\hat{k})}x^{\hat{k}}e^{-x}dx$ $\hat{\xi} = l_1 - \hat{k}\hat{\alpha}$

Source: Hamed and Rao (2019)

2.4 Accuracy Measure Performance

In this section, five accuracy performance measures are used which are Mean Absolute Error (MAE), Mean Absolute Percentage Error ($MAPE$), Root Mean Square Error ($RMSE$), Root Mean Square Percentage Error ($RMSPE$) and Coefficient of Determination (R^2). MAE is the mean of the absolute magnitude of differences between predicted and actual values irrespective of direction $MAPE$ generalizes this by quantifying errors in percentage terms, thus it can be used to compare across different magnitudes of floods. $RMSE$ conveys bigger errors by squaring the differences before computing the mean, thus it proves useful in identifying poorer predictions of the larger flood events. Lastly, $RMSPE$ is a percentage version of $RMSE$, but is better suited to evaluate predictions that vary greatly in magnitude, such as those for a number of floods return periods. The R^2 determine how well the theoretical estimated value derived from distribution fits the actual data. The smallest error measure and larger value of R^2 implies that the data perform better for the model. Hence, the equation of each accuracy performance is presented in Eq. (14) through Eq. (18).

https://doi.org/10.24191/jcrinn.v10i2.527

$$MAE = \frac{1}{n}\sum_{i=1}^{n}\left|F(y_i) - F(\hat{y}_i)\right| \tag{14}$$

$$MAPE = \frac{100}{n}\sum_{i=1}^{n}\left|\frac{F(y_i) - F(\hat{y}_i)}{F(y_i)}\right| \tag{15}$$

$$RMSE = \sqrt{\frac{\sum_{i=1}^{n}\left(F(y_i) - F(\hat{y}_i)\right)^2}{n}} \tag{16}$$

$$RMSPE = \sqrt{\frac{1}{n}\sum_{i=1}^{n}\left(\frac{F(y_i) - F(\hat{y}_i)}{F(y_i)}\right)^2} \times 100 \tag{17}$$

$$R^2 = \frac{\sum_{i=1}^{n}\left(F(\hat{y}_i) - F(y_i)\right)^2}{\sum_{i=1}^{n}\left(F(\hat{y}_i) - F(y_i)\right)^2 + \sum_{i=1}^{n}\left(F(y_i) - F(\hat{y}_i)\right)^2} \tag{18}$$

where n is the number of observations, $F(y_i)$ is the observed value, $F(\hat{y}_i)$ represented the predicted value, $\bar{y}$ is the mean of the observed value. The accuracy measurements such as $MAE, MAPE, RMSE$ and $RMSPE$ quantify the differences between the actual observation of annual peak flow and predicted estimates of peak flow from each distribution.

2.5 L-Moment ratio diagram

Hosking and Wallis (1997) introduced the L-Moment Ratio Diagram (LMRD) as a tool for calculating an accurate distribution of a catchment's streamflow series. Regarding a three-parameter distribution, the LMRD depicts the theoretical relationship between t_3 (skewness) and t_4 (kurtosis), as given in Eq. 12 and Eq. 13 respectively. The value of t_4 is calculated based on the Kahang River streamflow data and plot LMRD in order to recognize which distribution line lies closely.

$$\begin{aligned} t_4 = {} & A_0 + A_1 t_3 + A_2 (t_3)^2 + A_3 (t_3)^3 + A_4 (t_3)^4 + A_5 (t_3)^5 + A_6 (t_3)^6 \\ & + A_7 (t_3)^7 + A_8 (t_3)^8 \end{aligned} \tag{19}$$

The coefficients of A_k where $k=0, 1, 2, \ldots, 8$ for the GLO, GPA and PE3 respectively are from the L-Moment. To measure the distance between observed and predicted values for each distribution, Euclidean Distance can be used. This is to strengthen the graphical evidence on which distribution is the best. Hence, the formula for Euclidean Distance (Krislock & Wolkowicz, 2012) is expressed by:

$$d(p,q) = \sqrt{\sum_{i=1}^{n}\left(q_i - p_i\right)^2} \tag{20}$$

where q_i and p_i is the Euclidean vectors, starting from the origin of the space (initial point). For Euclidean distance, the smallest distance from the baseline indicates better model performance.

https://doi.org/10.24191/jcrinn.v10i2.527

3. RESULT AND DISCUSSION

Maximum streamflow also closely related with flooding engineering, flood management measurement development and flood system facilities drainage system. Table 1 summarized the descriptive statistics of Kahang River site's annual peak flow data from 1978 until 2022. It exhibits a mean peak flow of 280.41, higher than its median (193.95), indicating a right-skewed distribution with substantial variability. This large spread between the mean and median, coupled with a high standard deviation (262.633) with min (54.8) and max (1284.8), confirms the presence of extreme flow events in the dataset.

Table 2. Descriptive Statistics for Annual Streamflow of Kahang River

Station	n	Mean	SD	Min	Max	Skewness	Kurtosis
Kahang River	45	280.41	262.63	54.8	1284.8	2.00	3.87

The peak flow data for the Kahang River has a skewness of 2.0, suggesting that the data is skewed to the right with more frequent lower and occasional high peaks. The positive value of kurtosis suggests a leptokurtic (Kurtosis > 3.0), indicate that a higher likelihood of extreme flow events. Therefore, the results confirms that the peak flow data does not follow normal distribution but instead has heavy tail. To better capture this behavior, the study uses three non-normal probability distributions which are Generalized Logistic (GLO), Generalized Pareto (GPA) and Pearson Type-III (PE3) to model the annual maximum flows in Johor. Their parameters were estimated by applying the L-Moment, with the results listed in Table 3. To visualize the observed annual peak flow data, the Gringorton Plotting Position equation was used, as illustrated in Fig. 2.

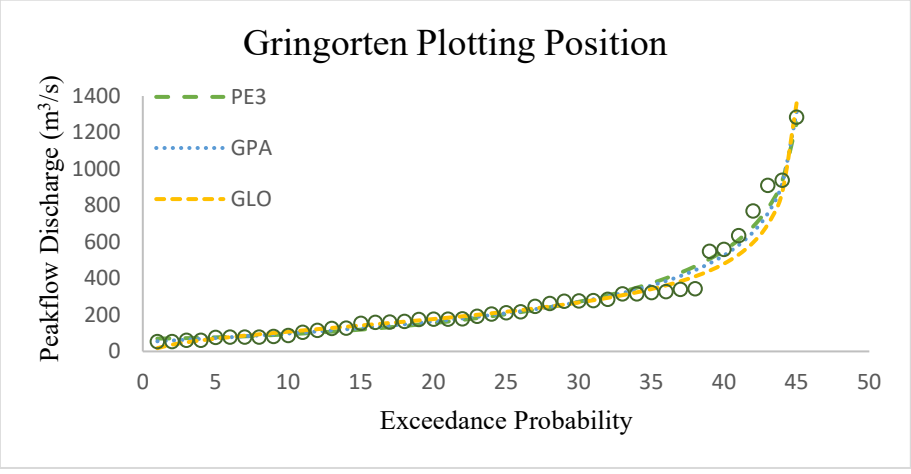

Fig. 2. CDF plot for the Kahang River annual peak flow and the candidate distributions

Fig. 2 shows all three distributions which are PE3, GLO and GPA which closely follow the observed data in the lower and central parts of the distribution, accurately capturing the general pattern of peak flows. However, in the upper tail region, where high discharge values are critical for flood risk assessments, there is a visible divergence among the models. While PE3 shows a slightly higher estimation, GPA tends to follow the observed data more consistently than GLO as the discharge increases. This suggests that GPA may be better at representing extreme events in this case, which is vital information when considering flood risk management and infrastructure design.

https://doi.org/10.24191/jcrinn.v10i2.527

Table 3. Estimated distribution parameters using the L-Moment technique

Distributions	Parameters		
	$\hat{\xi}$	$\hat{\alpha}$	$\hat{k}$
GLO	200.5983432	91.6763304	-0.4226313
GPA	53.2113263	184.416994	-0.1883087
PE3	280.412222	268.525419	2.553943

Table 3 displays the the estimated parameters for GLO, GPA, and PE3 distributions by employing the L-Moment technique. The GLO distribution has a central tendency (ξ) of 200.5983, the lowest variability (α) at 91.6763, and a negative skewness (k), indicating left-skewed data with more frequent low flood values. The GPA distribution has a much lower central tendency (ξ = 53.2113), higher variability (α = 184.4169), and mild left-skewness (k = -0.1883). In contrast, the PE3 distribution has the highest central tendency (ξ = 280.4122) and variability (α = 268.5254), with positive skewness (k = 2.5539), indicating right-skewed data and a higher likelihood of extreme flood magnitudes compared to GLO and GPA (Hamed & Rao, 2019).

Table 4. Performance measurement for candidate distributions

Distribution	GLO	GPA	PE3
MAE	29.23121014	23.89130881	25.91029352
MAPE	0.102461202	0.080253432	0.110348838
RMSE	53.52337859	40.20421989	39.08422233
RMSPE	0.33820537	0.100496606	0.133524466
R^2	0.950932826	0.97390899	0.975573279

Table 4 represent the performance of GLO, GPA and PE3 distributions using various metrics. The GPA distribution has the lowest MAE (23.8913) and $MAPE$ (0.0803), indicating the most accurate predictions, while PE3 has the smallest $RMSE$ (39.0842), showing better handling of large errors. GPA also leads in $RMSPE$ (0.1005), outperforming GLO (0.3382) and PE3 (0.1335). However, PE3 has the highest R^2 (0.9756), suggesting it explains slightly more variance in flood data than GPA (0.9739) and GLO (0.9509). Overall, GPA excels in accuracy, while PE3 performs best in minimizing large errors and explaining variability.

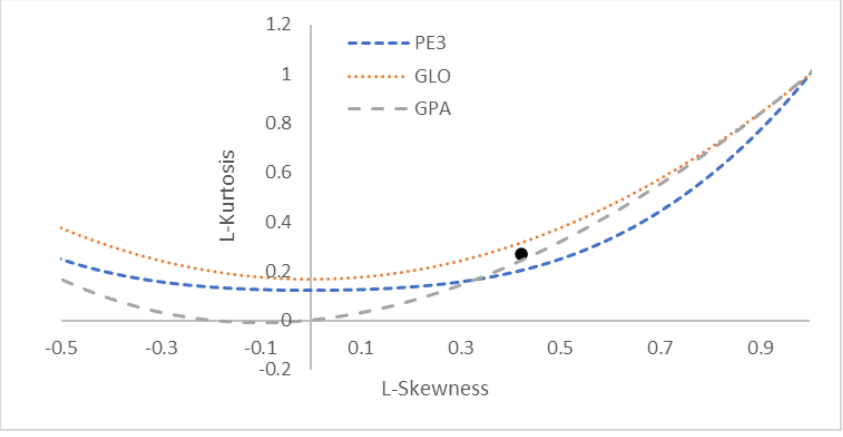

Fig. 3. L-moment ratio diagram

Fig. 3 displays the L-Moment Ratio Diagram (LMRD), comparing observed flood data which are plotted as a point with L-Skewness and L-Kurtosis = 0.2689 against theoretical curves of GLO, GPA and PE3 distributions. The observed point lies closest to the GPA curve, suggesting it may be the best fit, while

https://doi.org/10.24191/jcrinn.v10i2.527

GLO and PE3 show greater deviation. To objectively evaluate fit, the Euclidean distance measures how closely each distribution's theoretical values match the observed data, providing a quantitative goodness-of-fit comparison between the three distributions.

Table 5. Euclidean distance for each distribution

Distribution	Euclidean Distance
GLO	0.04480754
GPA	0.028652209
PE3	0.0666223

Table 5 presents the Euclidean distance results comparing the fit of GLO, GPA, and PE3 distributions to the observed flood data. The GPA distribution demonstrates the strongest alignment with the smallest distance (0.0287), confirming it as the most accurate model for this dataset. The GLO distribution, while reasonable with a distance of 0.0448, falls short of GPA's precision. In contrast, the PE3 distribution shows the poorest fit (0.0666), indicating it is the least suitable option among the three. These results clearly prioritize GPA as the optimal choice for modelling flood events at this location, balancing theoretical suitability with empirical performance.

Table 6. Rank score for candidate distributions

Distribution	GLO	GPA	PE3
MAE	1	3	2
MAPE	2	3	1
RMSE	1	2	3
RMSPE	1	3	2
R^2	1	2	3
Euclidean Distance	2	3	1
Total Score	11	20	14

Table 6 ranks the candidate distributions (GLO, GPA, PE3) using a scoring system. For each test and measure, the best distribution gets 3 points, the worst gets 1, and the middle performer gets 2. The scores are totaled and the distribution that hold the maximum overall score is chosen as the most fit, showing the most reliable performance across all evaluations. The GPA distribution emerges as the best choice for flood frequency modeling in Johor's river systems. It excels in accuracy measures ($MAE, MAPE, RMSPE, R^2$) and has the smallest Euclidean Distance. With the highest total rank score in Table 6, GPA outperforms GLO and PE3, which showed weaker results. This consistent superiority across all tests confirms GPA as the most reliable option for flood risk assessment in the Johor River.

Table 7. Estimated flood discharge for the Johor River site

Return Periods (Years)	Probability (p)	Estimated Flood Discharges (m^3/s)		
		GLO	GPA	PE3
2	0.50	200.5983	189.757	182.494
10	0.90	532.7005	584.7902	614.3538
50	0.98	1107.315	1119.669	1102.259

Table 7 gives the return period estimate for each distribution. From the table above, the flood discharge estimates from the GPA distribution increase with longer return periods (2, 10, 50 and 100 years). For 2 years (p = 0.50), it's 189.757 m³/s, rising to 584.790 m³/s (10 years, p = 0.90), 1119.669 m³/s (50 years, p = 0.98), and reaching 1404.908 m³/s for 100-year events (p = 0.99). This trend demonstrates GPA's effectiveness in modeling higher flood magnitudes for rare, extreme event.

https://doi.org/10.24191/jcrinn.v10i2.527

4. CONCLUSION

The FFA is a widely recognized hydrologic engineering approach that has gained significant interest among researchers. This study focuses on identifying the most fitted probability distribution for the modelling of the annual peak flow data at a Kahang river site in Johor, Malaysia using the L-moment method for parameter estimation, L-moment ratio (LMR) analysis, and numerical performance criteria. The analysis relied on annual maximum flow data from the Kahang River's historical records. By employing multiple assessment tools, the study ensures the chosen distribution is reliable for predicting return periods. Results indicate that the GPA distribution best fits the annual peak flow data for this site, making it a strong candidate for both regional and local FFA applications in Johor's River systems for future research.

5. ACKNOWLEDGEMENTS/FUNDING

The authors acknowledged the financial support from the Ministry of Higher Education Malaysia through Fundamental Research Grant Scheme FRGS-EC/1/2024/STG06/UITM/02/12.

6. CONFLICT OF INTEREST STATEMENT

The authors agree that this research was conducted in the absence of any self-benefits, commercial or financial conflicts and declare the absence of conflicting interests with the funders.

7. AUTHORS' CONTRIBUTIONS

Nur Hanida Othman: Conceptualization, Methodology, Formal analysis, Writing – original draft; **Basri Badyalina**: Supervision, Writing – review & editing, Validation, Project administration; **Ani Shabri**: Methodology, Validation, Resources, Writing – review & editing; **Muhammad Fadhil Marsani**: Data curation, Software, Visualization; **Fatin Farazh Ya'acob**: Investigation, Literature review, Data interpretation.

8. REFERENCES

Adhami, M. (2024). Regional flood frequency analysis of Northern Iran. *Dokuz Eylül Üniversitesi Mühendislik Fakültesi Fen ve Mühendislik Dergisi*, *26*(77), 272-280. https://doi.org/10.21205/deufmd.2024267711

Ahmad, N. F., Fakhru'l-Razi, A., mat said, A., Azan, R., & Muhaimin, R. (2020). Community preparedness to flood disaster in Johor, Malaysia. *IOP Conference Series: Earth and Environmental Science*, *479*(1), 012015. https://doi.org/10.1088/1755-1315/479/1/012015

Ali, S. & Rahman, A. (2022). Development of a kriging-based regional flood frequency analysis technique for South-East Australia. *Natural Hazards*, *114*(3), 2739-2765. https://doi.org/10.1007/s11069-022-05488-4

Badyalina, B., Mokhtar, N. A., Mat Jan, N. A., Hassim, N. H. & Yusop, H. (2021). Flood frequency analysis using L-moment for Segamat river. *Matematika*, *37*(2), 47-62. https://doi.org/10.11113/matematika.v37.n2.1332

Badyalina, B., Shabri, A., & Marsani, M. F. (2021). Streamflow estimation at ungauged basin using modified group method of data handling. *Sains Malaysiana*, *50*(9), 2765-2779. https://doi.org/10.17576/jsm-2021-5009-22

Badyalina, B., Mokhtar, N. A., Ya'acob, F. F., Ramli, M. F., Majid, M., & Jan, N. A. M. (2022). Flood frequency analysis using L-moments at Labis in Bekok river station. *Applied Mathematical Sciences*, *16*(11), 529-536. https://doi.org/10.12988/ams.2022.917192

Che Ilias, I. S., Wan Zin, W. Z. & Jemain, A. A. (2021). Regional frequency analysis of extreme precipitation in Peninsular Malaysia, In *e-Proceedings of the 5th International Conference on Computing, Mathematics and Statistics (iCMS 2021)* (pp. 160-172).

Fakhru'l-Razi, A., Diyana, F. A. N., Aini, M. S., Azan, R. A. & Muhaimin, R. W. M. (2020). Community preparedness to flood disaster in Johor, Malaysia. *IOP Conference Series: Earth and Environmental Science*, *479*(1), 012015. https://doi.org/10.1088/1755-1315/479/1/012015

Gringorten, I. I. (1963). A plotting rule for extreme probability paper. *Journal of Geophysical Research (1896-1977)*, *68*(3), 813–814. https://doi.org/https://doi.org/10.1029/JZ068i003p00813

Hamed, K. & Rao, A. Ramachandro. (2019). *Flood frequency analysis*. CRC press. https://doi.org/10.1201/9780429128813

Hassim, N. H., Badyalina, B., Mokhtar, N. A., Abd Jalal, M. Z. H., Zamani, N. D. B., Kerk, L. C. & Shaari, N. F. (2022). In situ flood frequency analysis used for water resource management in Kelantan River basin. *International Journal of Statistics and Probability*, *11*(5). https://doi.org/10.5539/ijsp.v11n5p8

Hosking, J. R. M. (1990). L-moments: analysis and estimation of distributions using linear combinations of order statistics. *Journal of the Royal Statistical Society: Series B: Statistical Methodology, 52*(1), 105–124. https://doi.org/10.1111/j.2517-6161.1990.tb01775.x

Hosking, J. R. M. & Wallis, J. R. (1997). Regional frequency analysis. In J. R. M. Hosking & J. R. Wallis (Eds.), *Regional Frequency Analysis: An Approach Based on L-Moments* (pp. 1-13). Cambridge University Press. https://doi.org/10.1017/CBO9780511529443.003

Jafry, N. A., Suhaila, J., Yusof, F., Nor, S. R. M. & Alias, N. E. (2023). Bivariate copula for flood frequency analysis in Johor River basin. *IOP Conference Series: Earth and Environmental Science*, *1167*(1), 012018. https://doi.org/10.1088/1755-1315/1167/1/012018

Jan, N. A. M., Shabri, A., Ismail, S., Badyalina, B., Abadan, S. S., & Yusof, N. (2016). Three-parameter lognormal distribution: Parametric estimation using L-moment and TL-moment approach. *Jurnal Teknologi (Sciences & Engineering)*, *78*(6-11). https://doi.org/10.11113/jt.v78.9202

Krislock, N., & Wolkowicz, H. (2012). Euclidean distance matrices and applications. In *Handbook on semidefinite, conic and polynomial optimization* (pp. 879-914). Springer. https://doi.org/10.1007/978-1-4614-0769-0_30

Landwehr, J. M., Matalas, N. C. & Wallis, J. R. (1979). Probability weighted moments compared with some traditional techniques in estimating gumbel parameters and quantiles. *Water Resources Research*, *15*(5), 1055–1064. https://doi.org/10.1029/WR015i005p01055

Linsley, R. K. (1986). Flood estimates: How good are they?. *Water Resources Research*, *22*(9S), 159S-164S. https://doi.org/10.1029/WR022i09Sp0159S

Marsani, M. F., Shabri, A., Badyalina, B., Jan, N. A. M., & Kasihmuddin, M. S. M. (2022). Efficient market hypothesis for Malaysian extreme stock return: Peaks over a threshold method. *Matematika,* 141-155. https://doi.org/10.11113/matematika.v38.n2.1396

Moughamian, M. S., McLaughlin, D. B. & Bras, R. L. (1987). Estimation of flood frequency: An evaluation of two derived distribution procedures. *Water Resources Research*, *23*(7), 1309–1319. https://doi.org/10.1029/WR023i007p01309

https://doi.org/10.24191/jcrinn.v10i2.527

Romali, N. S. & Yusop, Z. (2017). Frequency analysis of annual maximum flood for Segamat river. In *MATEC Web of Conferences*, EDP Sciences, *103,* 04003. https://doi.org/10.1051/matecconf/201710304003

Stedinger, J. (1993). Frequency analysis of extreme events. *Handbook of Hydrology*, 18.

Todd, D. K. (1957). Frequency Analysis of Streamflow Data. *Journal of the Hydraulics Division*, *83*(1), 1166-1-1166–18. https://doi.org/10.1061/JYCEAJ.0000060

Turhan, E. (2022). An investigation on the effect of outliers for flood frequency analysis: The case of the Eastern Mediterranean Basin, Turkey. *Sustainability*, *14*(24), 16558. https://doi.org/10.3390/su142416558

Valentini, M. H. K., Beskow, S., Beskow, T. L. C., de Mello, C. R., Cassalho, F. & da Silva, M. E. S. (2024). At-site flood frequency analysis in Brazil. *Natural Hazards*, *120*(1), 601–618. https://doi.org/10.1007/s11069-023-06231-3

Zamani, N. D., Badyalina, B., Jalal, A., Hakim, M. Z., Mohamad Khalid, R., Ya'acob, F. F. & Chang, K. L. (2024). Assessing flood risk using L-Moments: An analysis of the generalized logistic distribution and the generalized extreme value distribution at Sayong River Station. *Mathematical Sciences and Informatics Journal (MIJ)*, *5*(2), 105–115.

Zhang, J.-M., Chen, X.-H. & Ye, C.-Q. (2012). Calculation of negative-skewness hydrological series with Pearson-III frequency curve. *Journal of Hydraulic Engineering*, *43*(11), 1296–1301. https://doi.org/10.1061/(ASCE)HE.1943-5584.0000580

https://doi.org/10.24191/jcrinn.v10i2.527